Competition between symmetry breaking and onset of collapse in weakly coupled atomic condensates

L. Salasnich[1], B.A. Malomed[2] and F. Toigo[1]
[1] *CNISM and CNR-INFM, Unità di Padova, Dipartimento di Fisica "G. Galilei", Università di Padova, Via Marzolo 8, 35131 Padova, Italy*
[2] *Department of Physical Electronics, School of Electrical Engineering, Faculty of Engineering, Tel Aviv University, Tel Aviv 69978, Israel*

We analyze the symmetry breaking of matter-wave solitons in a pair of cigar-shaped traps coupled by tunneling of atoms. The model is based on a system of linearly coupled nonpolynomial Schrödinger equations (NPSEs). Unlike the well-known spontaneous-symmetry-breaking (SSB) bifurcation in coupled cubic equations, in the present model the SSB competes with the onset of collapse in this system. Stability regions of symmetric and asymmetric solitons, as well as the collapse region, are identified in the parameter space of the system.

PACS numbers: 03.75.Lm, 05.45.Yv, 42.65.Tg

Introduction. It is commonly known that the Gross-Pitaevskii equation (GPE) furnishes a very accurate description of the Bose-Einstein condensation (BEC) in rarefied gases of bosonic atoms [1]. One important applications of the GPE is the prediction of Josephson oscillations [2] and *spontaneous symmetry breaking* (SSB), alias macroscopic quantum self-trapping [3], in double-well potentials (DWPs). Experimentally, the oscillations [4, 5] and self-trapping [5] have been demonstrated in BECs with repulsive interactions between atoms, see Ref. [6] for a review. Asymmetric stationary states trapped in the DWP are generated by symmetry-breaking bifurcations from symmetric or antisymmetric states, in case the intrinsic nonlinearity is attractive or repulsive, respectively [3]. In fact, this bifurcation was first predicted (for the self-focusing nonlinearity) in the model of dual-core nonlinear optical fibers [7].

A natural extension of the DWP is a double-channel structure in the two-dimensional (2D) geometry, based on two potential wells in one direction (x), which are uniformly extended, as parallel troughs, in the perpendicular direction (z) [8, 9]. With the attractive cubic nonlinearity, this structure gives rise to double-hump solitons, which are supported by the DWP in the direction of x, while being self-trapped along z, as the ordinary matter-wave solitons in the cigar-shaped (single-core) trap [10]. Similarly shaped gap solitons were predicted in the double-channel model with the self-repulsive nonlinearity and a periodic potential (an optical lattice, OL) acting along z [9, 11]. If the nonlinearity is strong enough, an obvious symmetric/antisymmetric soliton in the double-channel setting with the self-attraction/repulsion may bifurcate into an asymmetric mode. This was demonstrated both in the full 2D models [8, 11] and their 1D counterparts, which replace the single 2D GPE by a pair of 1D equations with coordinate x, for wave functions in the two potential troughs, while the tunneling between the troughs in the x direction is approximated by a linear coupling between the 1D GPEs [9]. For the attractive nonlinearity, the system of 1D GPEs is identical to the model of dual-core nonlinear optical fibers with anomalous group-velocity dispersion, where the symmetry-breaking bifurcation and asymmetric solitons generated by it have been studied in detail [12, 13]. The difference between the linearly-coupled models with the intrinsic attraction and repulsion is in the character of the SSB bifurcation, which is *subcritical* and *supercritical* in the former and latter cases, respectively. The subcritical bifurcation gives rise to a narrow region of the bistability, where stable symmetric and asymmetric solitons coexist [12].

The DWP may also be extended in two transverse directions, forming a pair of parallel pancakes-shaped traps. The model developed for this setting is based on a pair of linearly-coupled 2D GPEs, which give rise to the SSB of 2D solitons and solitary vortices, for either sign of the nonlinearity, provided that the model includes an in-plane OL potential (otherwise, all 2D solitons are unstable) [14].

The analyses of the SSB in solitons, reported in previous works, were dealing with the cubic nonlinearity, except for Ref. [15], which considered a system of coupled equations combining the cubic attractive and quintic repulsive terms – a setting relevant to optics, rather than to BEC. It was demonstrated that the bifurcation diagrams, accounting for the SSB of solitons in that system, form a closed loop, unlike open diagrams generated by the cubic nonlinearity. An essential aspect of the description of BEC in the low-dimensional setting is that the reduction of the GPE from 3D to 1D transforms the original cubic nonlinearity into a *nonpolynomial* form [16, 17]. In the case of the self-attraction, the respective *nonpolynomial nonlinear Schrödinger* equation (NPSE) predicts the occurrence of collapse at a critical value of the density, in agreement with the underlying 3D cubic GPE [16]. The objective of this work is to study a hitherto unexplored aspect of the SSB in solitons, *viz.*, the competition between the SSB and the onset of the collapse, in the framework of a system of linearly coupled NPSEs (in Refs. [14], the possibility of the collapse of asymmetric solitons in

the 2D dual-core model with the attractive cubic nonlinearity and OL potential was mentioned, but not investigated, as the SSB happened there at much lower values of the density than those necessary for the onset of the collapse). Below, we derive the NPSE system, and then produce a diagram in its parameter space, which reveals regions of stable symmetric and asymmetric solitons and a collapse area.

The model. The starting point of the analysis is the scaled 3D GPE for the mean-field wave function, ψ, which describes the BEC in two parallel identical cigar-shaped traps separated by a potential barrier:

$$i\psi_t = \frac{1}{2}\left\{-\nabla^2 + \Omega^2\left[(x-a)^2 + (x+a)^2 - 4a^2 + y^2\right]\right\}\psi + W(z)\psi - 2\pi g\left|\psi\right|^2\psi, \quad (1)$$

where z is the longitudinal coordinate, $W(z)$ is the axial potential (if any), y is directed perpendicular to the plane drawn through axes of the parallel traps, x lies in the plane, being orientated perpendicular to the axes, and $2a$ is the distance between them. The coefficient $2\pi g > 0$ accounts for the attraction between atoms, and Ω^2 – for the transverse isotropic trapping in each "cigar".

Our first objective is to reduce Eq. (1) to a system of linearly coupled 1D equations. To this end, we modify the approach developed for the single "cigar" [16], adopting a superposition of two single-core *ansätze*:

$$\psi(x,y,z,t) = \frac{1}{\sqrt{\pi}}\left[\exp\left(-\frac{(x-a)^2+y^2}{2\sigma_1^2}\right)\frac{f_1(z,t)}{\sigma_1} + \exp\left(-\frac{(x+a)^2+y^2}{2\sigma_2^2}\right)\frac{f_2(z,t)}{\sigma_2}\right]. \quad (2)$$

Here f_1 and f_2 are the 1D (axial) wave functions in the two cores, and $\sigma_{1,2}$ are the respective transverse widths.

We proceed by substituting ansatz (2) into the energy functional (Hamiltonian) corresponding to Eq. (1),

$$E = \frac{1}{2}\int\int\int dxdydz\left\{\left|\nabla\psi\right|^2 + \Omega^2\left[(x-a)^2 + (x+a)^2 - 4a^2 + y^2\right]\left|\psi\right|^2 + 2W(z)\left|\psi\right|^2 - 2\pi g|\psi|^4\right\}. \quad (3)$$

The underlying assumption, that the distance between the "cigars" is essentially larger than the radius of the transverse confinement in each of them, implies $a^2\Omega \gg 1$. Due to this condition, the coupling energy, which is produced by the overlap of the two components of the wave function in ansatz (2), if substituted into Hamiltonian (3), takes the following form, for $\sigma_1 = \sigma_2 \equiv \sigma$: $E_{\rm coupl} = -\kappa\int_{-\infty}^{+\infty}\left[f_1(z)f_2^*(z) + f_1^*(z)f_2(z)\right]dz$, where $\kappa \equiv 2\left(a\Omega\right)^2\exp\left(-a^2/\sigma^2\right)$. The main contribution to $E_{\rm coupl}$ comes from region $x^2, y^2 \lesssim \sigma^2$ around the midpoint between the "cigars". In that region, the transverse- confinement radius is determined by the ground-state wave function of the 2D harmonic oscillator, i.e., $\sigma = \Omega^{-1/2}$, hence the coupling coefficient becomes a constant, $\kappa = 2\left(a\Omega\right)^2\exp\left(-a^2\Omega\right)$.

Other terms in Hamiltonian (3) are calculated separately for f_1 and f_2. The eventual result is (from now on, we set $\Omega \equiv 1$ by means of an obvious rescaling)

$$E = (1/2)\sum_{n=1,2}\int_{-\infty}^{+\infty}\left\{\left(\sigma_n^{-2} + \sigma_n^2 + 2W(z)\right)\left|f_n(z)\right|^2 + \left|\partial f_n/\partial z\right|^2 - g\sigma_n^{-2}\left|f_n(z)\right|^4\right\}dz - \kappa\int_{-\infty}^{+\infty}\left[f_1(z)f_2^*(z) + f_1^*(z)f_2(z)\right]dz\,, \quad (4)$$

where, as usual [16], the z-dependence of σ_n is neglected. The transverse widths are determined by the variational equations, $\delta E/\delta\sigma_n = 0$, which leads to the same relations as in the single-core model: $\sigma_n^2 = \sqrt{1 - g\left|f_n\right|^2}$. The substitution of this into energy functional (4) casts it into the final form,

$$E = \int_{-\infty}^{+\infty}\left\{\left[\sum_{n=1,2}\left(\sqrt{1-g\left|f_n\right|^2} + W(z)\right)\left|f_n(z)\right|^2 + \frac{1}{2}\left|\frac{\partial f_n}{\partial z}\right|^2\right] - \kappa\left[f_1(z)f_2^*(z) + f_1^*(z)f_2(z)\right]\right\}dz. \quad (5)$$

The system of coupled NPSEs is derived from Hamiltonian (5) as $i\left(f_n\right)_t = \delta E/\delta f_n^*$, i.e.,

$$i\frac{\partial f_n}{\partial t} = -\frac{1}{2}\frac{\partial^2 f_n}{\partial z^2} + W(z)f_n + \frac{1-(3/2)\,g\left|f_n\right|^2}{\sqrt{1-g\left|f_n\right|^2}}f_n - \kappa f_{3-n}, \quad (6)$$

Note that the derivation of the equations for f_n from the Hamiltonian in the form of Eq. (4), and subsequent substitution of expressions $\sigma_n^2 = \sqrt{1-g\left|f_n\right|^2}$, leads to the same equations (6). Equations (6) conserve energy (5) and the total norm (number of atoms in the condensate), $N = \int_{-\infty}^{+\infty}\left(\left|f_1(z)\right|^2 + \left|f_2(z)\right|^2\right)dz \equiv N_1 + N_2$.

In the low-density limit, $g|f_{1,2}|^2 \ll 1$, Eqs. (6) reduce to 1D GPEs,

$$i\left(f_n\right)_t = -(1/2)\left(f_n\right)_{zz} + W(z)f_n - g|f_n|^2 f_n - \kappa f_{3-n}\,, \quad (7)$$

This system, with $g > 0$, and $W(z) = 0$, is tantamount to the model of the dual-core nonlinear optical fiber with the anomalous group-velocity dispersion, where the SSB of solitons with $f_1\left(z,t\right) = f_2\left(z,t\right)$ was studied in detail [12, 13]. In terms of the double-trap BEC model based on system (7) with the OL potential, $W(z) = \epsilon\cos(2kx)$, the SSB of regular solitons, for $g > 0$, and gap solitons, for $g < 0$, was studied in Ref. [9]. In the case of $g < 0$, the bifurcation actually breaks the *antisymmetry* of the two-component gap solitons with $f_1\left(z,t\right) = -f_2\left(z,t\right)$. In

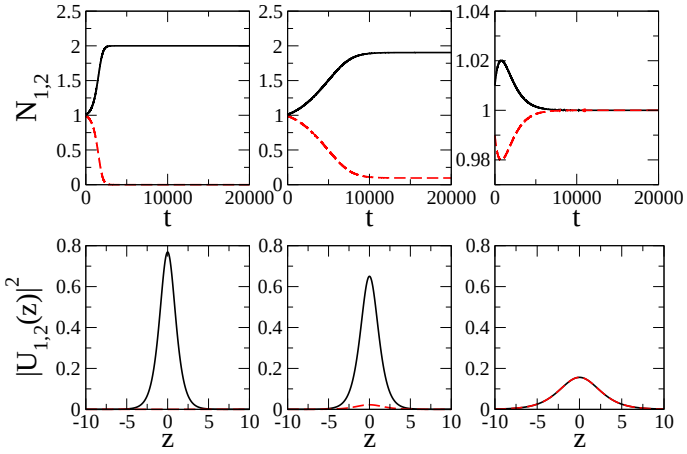

FIG. 1: (Color online). Upper panels: norms N_1 and N_2 (solid and dashed lines) in the course of the evolution in imaginary time. Lower panels: final density profiles of $U_1(z)$ and $U_2(z)$ (solid and dashed lines), corresponding to the cases shown in the upper panels. The nonlinearity coefficient is $g = 0.6$, while the coupling constant is $\kappa = 0$, 0.06, and 0.12, in the left, central, and right panels, respectively.

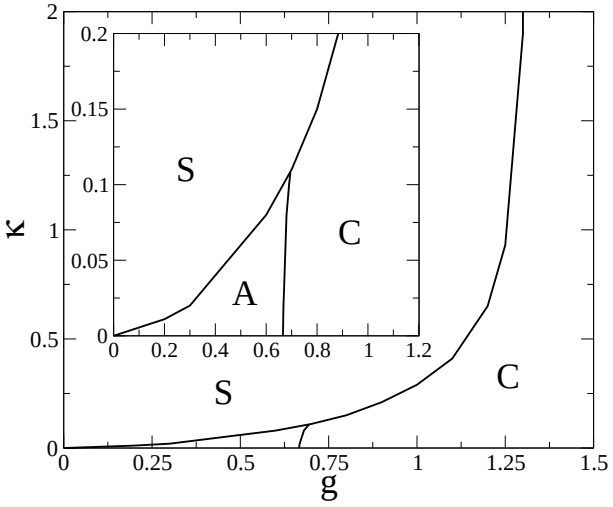

FIG. 2: The phase diagram of the linearly-coupled system of NPSEs in the parameter plane. In regions S and A, the system supports, respectively, stable symmetric $[U_1(z) = U_2(z)]$ and asymmetric $[U_1(z) \neq U_2(z)]$ stationary solutions. The collapse takes place in region C. The inset is a zoom of the area at small values of coupling constant κ, which shows the border between A and C in detail.

the present work, we focus on the model with the self-attraction, $g > 0$, when the difference of the nonlinearity in Eqs. (7) from the cubic form is important. As said above, the most interesting issue is the competition between the SSB and the onset of the collapse, which is admitted by the NPSE even in the framework of the 1D description [16].

Results. To specify the normalization for functions $f_{1,2}(z)$, we fix the total norm, $N_1 + N_2 \equiv 2$, while N_1 and N_2 may vary. Then, the full set of stationary solutions to Eqs. (6), $f_{1,2}(z,t) = e^{-i\mu t} U_{1,2}(x)$, with real functions $U_{1,2}(z)$ and chemical potential μ, is parameterized by two coefficients, g and κ. We integrated Eqs. (6) in imaginary time, using a finite-difference Crank-Nicolson code and imposing condition $N = 2$ at each step. Initial wave functions were taken as Gaussians with norms $N_1 = 1.01$ and $N_2 = N - N_1 = 0.99$.

In Fig. 1 we report typical examples of totally asymmetric, strongly asymmetric, and symmetric solitons found below the collapse threshold (at $g = 0.6$), for different values of the linear coupling κ. At $\kappa = 0$, wave function $f_1(z)$ with initial norm $N_1 = 1.01$ evolves into a single-component bright soliton which absorbs the total norm, $N = 2$, while $f_2(z)$, with initial norm $N_2 = 0.99$, decays to zero. At $\kappa = 0.06$ (weak linear coupling), the wave functions evolve into a stable two-component soliton with a strongly broken symmetry. Finally, the strong linear coupling, with $\kappa = 0.12$, enforces the evolution of the soliton into the symmetric form.

The collapse of wave function $f_1(z,t)$ occurs in simulations of system (6) with $\kappa = 0$ at $g \geq 2/3$, if the evolution commences with initial norm $N_1 = 1.01$. This result agrees with known properties of the single-component NPSE [16], assuming that the total norm, $N = 2$, goes to f_1. A suppression of the collapse takes place at finite values of κ. The results are summarized in Fig. 2, in the form of a diagram in the plane of (g,κ). It features three regions: stable symmetric and asymmetric solitons in S and A, respectively, and collapsing solutions in C. An obvious rescaling argument explains that all solutions suffer the collapse at any κ for $g \geq 4/3$, which is twice the above-mentioned critical value, $g = 2/3$, for the single-component system with $N = 2$. It corresponds to the symmetric collapse mode, with equal norms $N_1 = N_2 = 1$ in each trap. In accordance with these features, the border between regions A and C in Fig. 2 starts, at $\kappa = 0$, with $g = 2/3$, while the border between S and C asymptotes to $g = 4/3$ at large values of κ. Notice that in the inset of Fig. 2 the (A,C) border seems straight but it is actually curved, as shown in the main figure.

The SSB in solitons is characterized by the asymmetry parameter [9, 12], $\Theta = (N_1 - N_2)/(N_1 + N_2)$. The competition between the symmetry breaking and collapse is further illustrated in Fig. 3 by plots of Θ versus g for a relatively weak coupling. In the upper panel we fix $\kappa = 0.05$ and compare the usual model based on linearly coupled cubic GPEs, Eqs. (7), with the linearly coupled NPSEs, Eqs. (6). In the lower panel we plot the NPSE curves for three values of κ.

The diagrams of Fig. 3 feature a leap from the symmetric configuration with $\Theta = 0$ to the asymmetric one with $\Theta \neq 0$, cf. a similar situation in the 2D model considered in Ref. [8]. The transition to asymmetric states in the present model always happens by a leap, i.e., the symmetry-breaking bifurcation is always subcritical, similar to the situation in the coupled equations with the self-attractive cubic nonlinearity [12]. The SSB may be

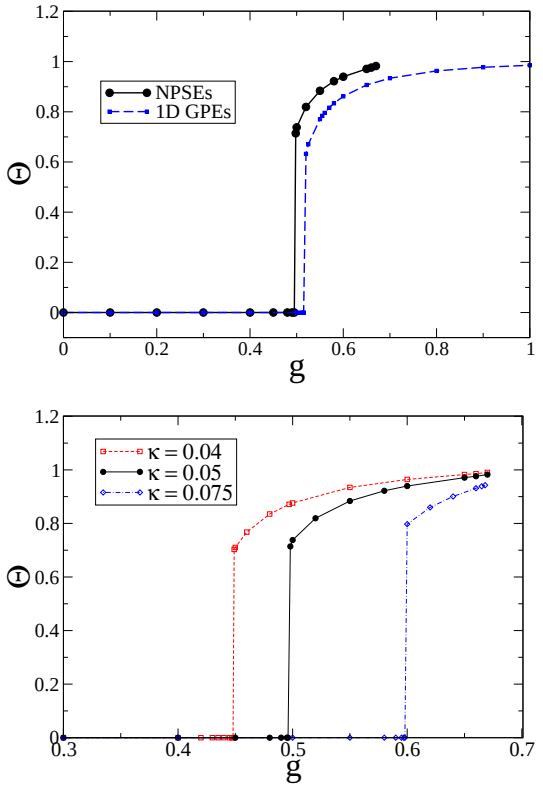

FIG. 3: (Color online). The asymmetry parameter, $\Theta = (N_1 - N_2)/(N_1 + N_2)$, as a function of interaction strength g. Upper panel: fixed $\kappa = 0.05$, as obtained from the coupled NPSEs (squares) and 1D GPEs, i.e., usual equations with the cubic nonlinearity. Lower panel: three values of the parameter κ; curves obtained with the coupled NPSEs. The lines corresponding to the NPSE system terminate at the collapse point.

considered as a first-order quantum (zero-temperature) phase transition, with Θ playing the role of the order parameter of the transition [18]. The main difference between the $\Theta(g)$ plots generated by Eqs. (6) and Eqs. (7) is the fact that the former system predicts the collapse of the asymmetric configuration at $g \approx 0.66$, while the cubic nonlinearity in the latter system does not give rise to any collapse. Lastly, it is seen from Fig. 2 that asymmetric solitons do not exist at $\kappa > \kappa_{\max} \approx 0.108$. Accordingly, with these values of the linear-coupling coefficient the SSB does not occur, and the collapse happens directly in the symmetric mode, at the above-mentioned critical value, $g = 4/3$.

Conclusion. The objective of this work was to explore the SSB in solitons described by the system of linearly coupled NPSEs. The difference from the soliton bifurcations in coupled cubic equations is that the SSB competes with the onset of the collapse. The phase diagram in the system's parameter plane was produced, revealing regions of stable symmetric and asymmetric solitons, and of the collapse as well. The symmetry-breaking bifurcation is subcritical, unless the collapse occurs before the SSB. It may be quite interesting to extend this model for the description of the SSB in a pair of parallel pancake-shaped traps, described by linearly coupled two-dimensional NPSEs.

This work was partially supported by Fondazione Cariparo (Padova, Italy). B.A.M. appreciates grant No. 149/2006 from the German-Israel Foundation.

[1] C. J. Pethick and H. Smith, *Bose–Einstein Condensation in Dilute Gases* (Cambridge University Press: Cambridge, 2002).
[2] J. Javanainen, Phys. Rev. Lett. **57**, 3164 (1986); S. Giovanazzi, A. Smerzi, and S. Fantoni, *ibid.* **84**, 4521 (2000); E. A. Ostrovskaya *et al.*, Phys. Rev. A 61, 031601(R) (2000); J. E. Williams, *ibid.* **64**, 013610 (2001); K. W. Mahmud, J. N. Kutz, and W. P. Reinhardt, *ibid.* **66**, 063607 (2002); M. O. Oktel and L. S. Levitov, *ibid.* **65**, 063604 (2002); E. Sakellari, N. P. Proukakis, M. Leadbeater, and C. S. Adams, New J. Phys. 6, 42 (2004); S. K. Adhikari, Phys. Rev. A **72**, 013619 (2005); P. Zin *et al.*, *ibid.* **73**, 022105 (2006); U. R. Fischer, C. Iniotakis, and A. Posazhennikova, *ibid.* **77**, 031602 (2008); F. Ancilotto, L. Salasnich, and Toigo, *ibid.* **79**, 033627 (2009).
[3] G. J. Milburn, J. Corney, E. M. Wright, and D. F. Walls, Phys. Rev. A **55**, 4318 (1997); A. Smerzi *et al.*, Phys. Rev. A **59**, 620 (1999).
[4] F. S. Cataliotti *et al.*, Science **293**, 843 (2001); T. Anker *et al.*, Phys. Rev. Lett. **94**, 020403 (2005); S. Levy, E. Lahoud, I. Shomroni, and J. Steinhauer, Nature **449**, 579 (2007).
[5] M. Albiez *et al.*, Phys. Rev. Lett. **95**, 010402 (2005).
[6] R. Gati and M. Oberthaler, J. Phys. B. **40**, R61 (2007).
[7] A. W. Snyder *et al.*, J. Opt. Soc. Am. B **8**, 2102 (1991).
[8] M. Matuszewski, B. A. Malomed, and M. Trippenbach, Phys. Rev. A **75**, 063621 (2007).
[9] A. Gubeskys and B. A. Malomed, Phys. Rev. A **75**, 063602 (2007).
[10] K. E. Strecker *et al.*, Nature **417**, 150 (2002); L. Khaykovich *et al.*, Science **256**, 1290 (2002).
[11] M. Trippenbach *et al.*, Phys. Rev. A 78, 013603 (2008).
[12] C. Paré and M. Fłorjańczyk, Phys. Rev. A **41**, 6287 (1990); P. L. Chu, B. A. Malomed, and G. D. Peng, J. Opt. Soc. Am. B **10**, 1379 (1993); B. A. Malomed, I. Skinner, P. L. Chu, and G. D. Peng, Phys. Rev. E **53**, 4084 (1996).
[13] N. Akhmediev and A. Ankiewicz, Phys. Rev. Lett. **70**, 2395 (1993); J. M. Soto-Crespo and N. Akhmediev, Phys. Rev. E **48**, 4710 (1993).
[14] A. Gubeskys and B. A. Malomed, Phys. Rev. A **76**, 043623 (2007); L. Gubeskys and B. A. Malomed, *ibid.* **79**, 045801 (2009); B. Julia-Diaz, D. Dagnino, M. Lewenstein, J. Martorell, and A. Polls, arXiv:0912.1239.

[15] L. Albuch and B. A. Malomed, Mathematics and Computers in Simulation **74**, 312 (2007).
[16] L. Salasnich, Laser Phys. **12**, 198 (2002); L. Salasnich, A. Parola, and L. Reatto, Phys. Rev. A **65**, 043614 (2002).
[17] A. M. Mateo and V. Delgado, Phys. Rev. A **74**, 065602 (2006); **75**, 063610 (2007).
[18] K. Huang, *Statistical Mechanics* (Wiley, New York, 1987).